PROCEEDINGS OF SCIENCE

Search for heavy axions with the European X-Ray Free Electron Laser

Subir Sarkar,[a,*] **Charles D. Arrowsmith,**[b] **Carsten Baehtz,**[c] **Konstantin A. Beyer,**[d] **Robert Bingham,**[e,f] **Sebastian Goede,**[g] **Gianluca Gregori,**[a] **Jack W. D. Halliday,**[e] **Charles Heaton,**[a] **Oliver Humphries,**[g] **Alejandro Laso Garcia,**[c] **Giacomo Marocco,**[c] **Motoaki Nakatsutsumi,**[g] **Richard Plackett,**[a] **Thomas R. Preston,**[g] **Ian Shipsey,**[a] **Pontus Svensson,**[a] **Georgios Vacalis,**[a] **Justin Wark,**[a] **Daniel Wood**[a] **and Ulf Zastrau**[g]

[a] *Department of Physics, University of Oxford, Parks Road, Oxford OX1 3PU, United Kingdom*
[b] *University of Rochester, Laboratory for Laser Energetics, Rochester, NY 14623, USA*
[c] *Helmholtz-Zentrum Dresden-Rossendorf, Bautzner Landstraße 400, 01328 Dresden, Germany*
[d] *Max-Planck-Institut für Kernphysik Saupfercheckweg 1, 69117 Heidelberg, Germany*
[e] *STFC, Rutherford Appleton Laboratory, Didcot OX11 0QX, UK*
[f] *John Anderson Building, University of Strathclyde, G4 0NG, UK*
[g] *European XFEL, Holzkoppel 4, 22869 Schenefeld, Germany*
[h] *Lawrence Berkeley National Laboratory, 1 Cyclotron Road, Berkeley, CA 94720-8153, USA*

E-mail: subir.sarkar@physics.ox.ac.uk

When the Peccei-Quinn symmetry breaks after inflation, domain walls will form at the QCD scale in the axion field if there is more than one quark charged under the symmetry (as in e.g. the DFSZ model). When destabilised by quantum gravity effects, the collapse of the wall network creates relativistic axions, which subsequently turn non-relativistic and contribute to cold dark matter. Accounting for this additional contribution then requires the axion to be heavier than 11 meV — a mass range that is little explored experimentally. We describe first results from a new light-shining-through-walls search for such heavy axions at the EuXFEL, Hamburg.

39th International Cosmic Ray Conference (ICRC2025)
15–24 July 2025
Geneva, Switzerland

*Speaker

PoS(ICRC2025)524

1. Introduction

The axion arises from the breaking of Peccei-Quinn (PQ) symmetry [1–3], which was proposed to explain the absence of CP-violation by the strong interactions as described by the theory of quantum chromodynamics (QCD). Axion-like particles (ALPs) also arise in string theory [4]. Although very light and with suppressed couplings, coherent oscillations of relic axions can naturally account for cold dark matter if $m_a \sim 10^{-6}$–10^{-4} eV [5–7]. Laboratory 'haloscope' searches for axions converting to photons in a magnetic field [8] have therefore focussed on this 'light axion window' [9], targeting axion-photon couplings corresponding to the Galactic halo dark matter being made of axions. This coupling is related (inversely) to the scale of PQ symmetry breaking in extensions of the Standard Model that implement the PQ symmetry, e.g. the Kim-Shifman-Vainshtein-Zakarov (KSVZ) model [10, 11] or the Dine-Fischler-Srednicki-Zhitnitsky (DFSZ) model [12, 13]. It has been noted that when the PQ symmetry breaks *after* cosmological inflation, axions are also produced by the decay of topological defects in the axion field viz. strings [14] and domain walls [15]. The preferred mass for axions to make up dark matter then exceeds 11 meV in the DFSZ model [16]. The corresponding scale of Peccei-Quinn symmetry breaking is then rather low, so is theoretically preferred as being less susceptible to the 'axion quality problem', viz. the potential destabilising effects of quantum gravity on global symmetries [17–20].

Stringent bounds on such 'heavy' axions (excluding astrophysical arguments based on stellar cooling [21]) come from the CERN Axion Solar Telescope (CAST) [22] — a 'helioscope' which looks for conversion of axions emitted by the Sun into X-ray photons as they pass through a strong magnetic field. Due to the specific experimental geometry of CAST, the axion-photon conversion probability gets highly suppressed for $m_a \gtrsim 1$ eV. For such masses, better bounds on the axion-photon coupling have been claimed from underground searches for dark matter and $\beta\beta$-decay by examining Bragg conversion in the electric field of crystals [23–30]. However when the damping of X-rays in a crystal is taken into account, such bounds are considerably weakened [31]. Moreover, since the axions come from the Sun there is model dependence in extracting such bounds; in particular the plasma frequency and temperature in the Sun can perturb the effective axion-photon coupling [21, 32]. Similarly bounds derived from stellar cooling arguments, e.g. neutrino observations of Supernova 1987a, have large astrophysical uncertainties [33], however consideration of axion emission by supernovae sets a model-independent bound of $m_a < 53^{+7.3}_{-1.3}$ meV [34].

By contrast in laboratory experiments the axion production process is directly controlled, avoiding any model dependence. Interesting constraints have been set by searches at accelerators, using NOMAD [35], BaBar [36, 37], and NA64 [38], although they do not presently have the same sensitivity as astrophysical arguments. Of course it is important to use as many different experimental approaches as possible, since each has its own characteristic strengths and limitations.

Here we present results from a new search for axions performed with the HED/HiBEF instrument at the EuXFEL in Hamburg [39], which is sensitive to a broad range of axion/ALP mass between $\sim 10^{-3} - 10^{4}$ eV. Our experiment exploits the Primakoff effect via which a photon can decay into an axion in the presence of another photon, provided by a strong external electric or magnetic field, and then reconvert back into a photon after passing through an opaque wall. This technique has been previously employed in 'light-shining-through-a-wall' experiments using optical lasers and external magnetic fields [40–42].

Using X-rays, it is possible to increase the axion conversion/detection sensitivity by exploiting the electric fields within a crystal which can be as high as 10^{11} V/m, corresponding to magnetic field strengths of $O(1)$ kT [43]. This is much higher than is obtainable using the best electromagnets, however the relevant length scales are much smaller so the path integrated equivalent field is comparable, being $\sim$ 25 Tm in the present study. Furthermore, arranging atoms in a crystalline structure leads to a coherent effect analogous to Bragg scattering; generation and reconversion can thus be carried out with a pair of X-ray crystals [44]. We improve on previous laboratory-based searches in the above mass range (up to 2.4 keV) performed using 3$^{\rm rd}$ generation synchrotron facilities [45, 47] by achieving higher detection sensitivity thanks to the increased brightness of a X-ray Free Electron Laser (XFEL). This is because of the much shorter duration of the photon pulse which allows for a more accurate discrimination of the signal against the background.

2. Experimental setup

We use the term axion to describe both the QCD axion and any ALP which couples to photons via the dimension-5 operator

$$\mathcal{L}_{\rm axion} = g_{a\gamma\gamma}\mathbf{E}\cdot\mathbf{B}\,a, \tag{1}$$

where $\mathbf{E} \equiv \mathbf{E}_{\rm eff}$ is the electric field in the crystal lattice, $\mathbf{B} \equiv \mathbf{B}_{\rm FEL}$ is the magnetic field associated with the electromagnetic wave of the X-ray photon, a is the CP-conserving scalar field of the axion, and $g_{a\gamma\gamma}$ is the axion-photon coupling.

Figure 1 shows our experimental setup, with 2 germanium (Ge) crystals oriented in Laue geometry with their lattice planes parallel to each other. The σ-polarised XFEL beam impinges on the first crystal from the left, with the angle between the wave-vector and the crystal lattice plane denoted θ. Note that the Laue geometry is preferable to the more conventional Bragg scattering geometry because of the Borrmann effect, due to which the transmission of X-rays in the Laue case is is significantly increased [44, 45].

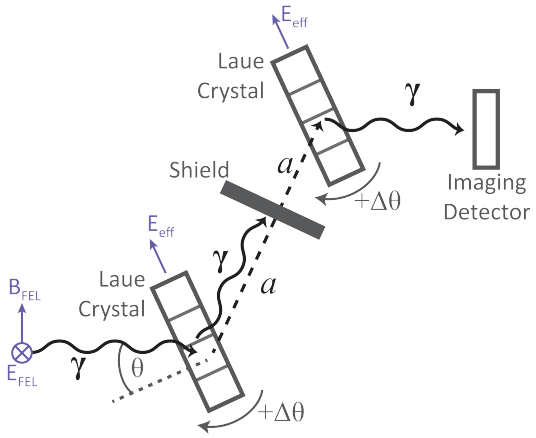

Figure 1: Diagram of the experimental setup. Axion production and photon regeneration take place via the effective electric field within a pair of Ge (220) monolithic crystals ($10 \times 10 \times 0.5$ mm) in Laue geometry, oriented by a pair of piezoelectric rotation stages (Xeryon, XRT-U30). The shield is a 1 mm thick Ti sheet. The X-ray beam polarisation maximises the value of $\mathbf{B}_{\rm FEL}\cdot\mathbf{E}_{\rm eff}$, hence the probability of axion production.

Both the generated axions (a) and Laue diffracted photons (γ) are transmitted through the first crystal. The photons are absorbed by the radiation shield but the weakly interacting axions penetrate and impinge on the second crystal where the strong electric field enables, via the inverse Primakoff process, the regeneration of photons which are observed by a detector downstream. When θ equals $\theta_{\rm B}$ (the Bragg angle), the design is sensitive to a broad range of axion mass satisfying the inequality

$$|m_a^2 - m_\gamma^2| \lesssim \frac{4k_\gamma}{L_{\rm eff}}, \tag{2}$$

where $m_\gamma = 44$ eV is the plasma frequency of the valence electrons in the conversion crystals [45]; k_γ is the photon energy; and $L_{\rm eff}$ is the effective path length of X-rays within a crystal.

When there is a detuning from the Bragg angle by $\Delta\theta = \theta - \theta_{\rm B}$, it can be shown [43, 45] that this setup becomes sensitive to a narrow range of axion mass ($\Delta m_a \sim 10^{-3}$ eV) centered on

$$m_a = \sqrt{m_\gamma^2 + 2q_{\rm T}k_\gamma \cos(\theta_{\rm B})\Delta\theta}, \tag{3}$$

where $q_{\rm T} = 6.20$ keV is the magnitude of the reciprocal lattice vector. Thus by sweeping through different values of $\Delta\theta$ we can search for axions with mass bracketed between the plasma frequency of the crystal and the projection of the incoming photon energy onto the reciprocal lattice vector.

The EuXFEL was operated in a seeded mode, with 9.8 keV photon energy (wavelength, $\lambda_{\rm x} = 2\pi/k_\gamma = 1.265$ Å). The repetition rate was 10 Hz, with one pulse per train. The X-ray beam was collimated by upstream compound refractive lenses (CRLs). The full-width-half-maximum of the beam transverse profile was measured to be 400 μm at the center of the interaction chamber. The axion-photon conversion probability $P(a \leftrightarrow \gamma)$ for Laue-case diffraction is given by [45]

$$P(a \leftrightarrow \gamma) = \left(\frac{1}{4} g_{a\gamma\gamma} E_{\rm eff}\, L_{\rm eff}\, \cos\theta_{\rm B}\right)^2, \tag{4}$$

where $E_{\rm eff} = 7.3 \times 10^{10}$ V/m is the crystalline electric field [45], and

$$L_{\rm eff} = 2L_{\rm att}^{\rm B}\left(1 - {\rm e}^{-L_{\rm x}/2L_{\rm att}^{B}}\right), \tag{5}$$

where $L_{\rm x} = \ell/\cos(\theta_{\rm B} + \Delta\theta)$ is the X-ray path length inside the crystals ($\ell = 500$ μm is the thickness of each crystal) and $L_{\rm att}^{\rm B} = 1499.8$ μm (for σ-polarization) [46]. However since the X-ray pulse duration in our experiment is short compared to that at a synchrotron facility, the result above requires modification. For a short (i.e. transform-limited) X-ray pulse, the width of the rocking curve ($\Delta\theta_{\rm RC}$) and timescale of the scattering process (Δt) form a time-bandwidth product given by: $\Delta\theta_{\rm RC}\Delta t \simeq \lambda_{\rm x} \tan\theta_{\rm B}/c$. Because of the Borrmann effect, the extinction length of the X-rays is longer than the X-ray path-length in the crystal, therefore the characteristic timescale is simply given by the geometric time-delay due to scattering off multiple planes: $c\Delta t = 2\ell \tan\theta_{\rm B} \sin\theta_{\rm B}$. Combining these expressions yields a rocking curve width $\Delta\theta_{\rm RC} \simeq 0.4$ µrad, which is far narrower than the Darwin width, $\Delta\theta_{\rm D} = 44$ µrad for Ge (220) [46]. This narrowing of the rocking curve may also be interpreted as a change in the effective index of refraction inside the crystal lattice [45].The interaction amplitude must then increase by a factor $\xi_{\rm B} = \Delta\theta_{\rm D}/\Delta\theta_{\rm RC}$, hence, the scattering probability becomes

$$P(a \leftrightarrow \gamma) \simeq \left(\frac{1}{4} g_{a\gamma\gamma} E_{\rm eff}\, L_{\rm eff}\, \xi_{\rm B}\, \cos\theta_{\rm B}\right)^2. \tag{6}$$

$\Delta\theta$ [mrad]	m_a [eV]	$N_{\rm in}$ ($\times 10^{16}$)	$g_{a\gamma\gamma}$ [eV]
0.0	$\lesssim 44$	2.6	3.91×10^{-4}
1.0	3.4×10^2	2.4	3.10×10^{-4}
1.8	4.6×10^2	1.6	3.87×10^{-4}
10.0	1.1×10^3	1.7	3.69×10^{-4}
50.0	2.4×10^3	1.5	2.76×10^{-4}

Table 1: inferred bound on the axion-photon coupling, $g_{a\gamma\gamma}$ for various detuning angles, $\Delta\theta$ and the corresponding mass, m_a; $N_{\rm in}$ is the total number of incident X-ray photons.

3. Results

The regenerated photons were measured using a silicon hybrid-pixel JUNGFRAU detector. Our search was limited to 5 discrete $\Delta\theta$ values, with data collected for 60 – 90 min at each angle. Table 1, shows the bounds on the axion-photon coupling determined at each detuning angle. Figure 2 shows energy-resolved events for each of the data sets in Table 1, compared against the number of counts in a 24-hour long dark run. The axion signal can be distinguished from the background as reconverted X-rays must be *identical* to the primary EuXFEL X-rays, and moreover must fall inside the region on the detector which is impacted by the X-ray beam when the shield is absent.

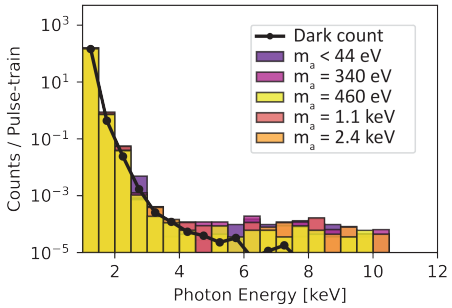

Figure 2: Events detected across all acquisitions, along with the number of counts in a 24 hour dark run.

To establish if any of the few events in the relevant energy band do fall upon the X-ray spot and might therefore be associated with axion production, hit-maps of events were produced as in Figure 3. The blue colour map shows transmission through the setup in the absence of the radiation shield while the overlaid data points indicate the location of hits on the detector with a photon energy exceeding 4 keV for each of the data sets in Table 1. It is seen that there are no events which overlap with the region of the X-ray spot (the darker blue region in the centre of the figure). Their absence implies that no events consistent with axion production were detected during the experiment. The corresponding limit on the axion-photon coupling is then obtained by inverting Eq. (6):

$$g_{a\gamma\gamma} < \left(\frac{1}{4} E_{\rm eff}\, L_{\rm B}\, \xi_B\, \cos\theta_{\rm B}\right)^{-1} P(a \leftrightarrow \gamma)^{1/2}, \tag{7}$$

with $P(a \leftrightarrow \gamma)^2 = (N_{\rm det}/\eta N_{\rm in})$, where $N_{\rm det}$ and $N_{\rm in}$ are the number of detected and incident photons. The efficiency factor η accounts for losses associated with the deviation from parallelism

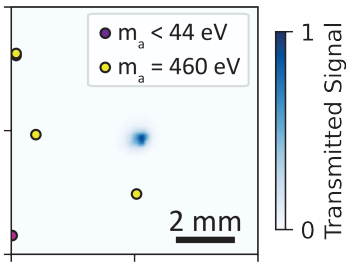

Figure 3: An image showing the transmitted signal in the absence of the radiation shield (blue colour-map) overlaid with the position of $k_\gamma \geq 4$ keV events across all data acquisitions.

between the two crystals; fluctuations in the exact X-ray energy; and the quantum efficiency of the detector. The value of η was obtained experimentally: At the beginning and end of each data run, the crystals were tuned to the Bragg angle and the radiation shield was removed in order to characterise the experimental setup.

The outcome of this analysis is shown in Figure 4 along with other bounds in the meV–keV mass range from searches for laboratory-generated axions. We were able to improve on the results from Ref. [47] at several discrete axion masses. For $m_a \gtrsim 200$ eV, we achieve a sensitivity within a factor 10 of previous searches, viz. NA64 [38] and BaBar [36, 37]. This is however not the best sensitivity achievable with the present setup which should be considered a 'proof-of-principle'. Issues with X-ray heating forced us to attenuate the X-ray flux by a factor of 10^3. Moreover, the X-ray bunch structure was set with the number of pulses per train limited to 1, out of a possible 300. Issues with retaining alignment also limited data acquisition time to 60-90 min at each detuning angle; with a more stable setup that would include active cooling of the first conversion crystal, these times could be increased by a factor of 30. Furthermore, we could also fully exploit the Borrmann effect and use Ge crystals up to 1.5 mm in thickness. Taken together these improvements would increase the sensitivity by a factor of ~ 150, bringing the estimated sensitivity down to 2×10^{-6} GeV^{-1}, which is close to the expectation for QCD axions.

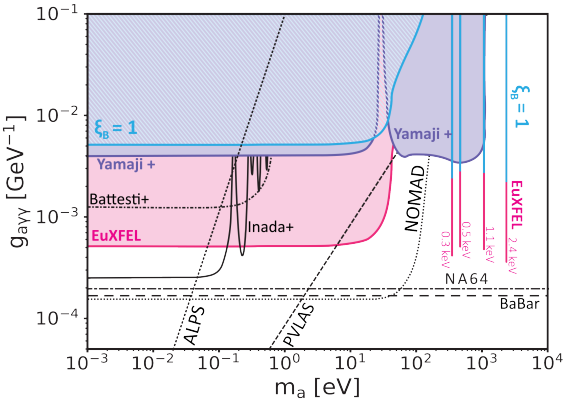

Figure 4: Bounds on the axion-photon coupling from our experiment (pink), compared with those from Yamaji et al. [45, 47] (purple). The excluded region (blue) taking $\xi_B = 1$ in Eq. (7) illustrates the improvement due to the higher photon number. Shown for comparison are other laboratory bounds: NOMAD [35], PVLAS [48], ALPS [41], NA64 [38], BaBar [36, 37], Battesti et al. [49] and Inada et al. [50].

Acknowledgements

This experiment was made possible by the efforts of my collaborators, led by our PI Gianluca Gregori. We acknowledge support from the UK Engineering & Physical Sciences Research Council (EP/X01133X/1) and the provision of beam time and assistance at the European XFEL. I am also grateful to my theory collaborator Konstantin Beyer for motivating the hunt for heavy axions.

References

[1] R. D. Peccei and H. R. Quinn, Phys. Rev. Lett. **38** (1977) 1440

[2] S. Weinberg, Phys. Rev. Lett. **40** (1978) 223

[3] F. Wilczek, Phys. Rev. Lett. **40** (1978) 279

[4] P. Svrcek and E. Witten, JHEP **06** (2006) 051

[5] J. Preskill, M. B. Wise and F. Wilczek, Phys. Lett. B **120** (1983) 127

[6] L. F. Abbott and P. Sikivie, Phys. Lett. B **120** (1983) 133

[7] M. Dine and W. Fischler, Phys. Lett. B **120** (1983) 137

[8] P. Sikivie, Phys. Rev. Lett. **51** (1983) 1415 [erratum: Phys. Rev. Lett. **52** (1984) 695]

[9] Y. K. Semertzidis and S. Youn, Sci. Adv. **8** (2022) abm9928

[10] J. E. Kim, Phys. Rev. Lett. **43** (1979) 103

[11] M. A. Shifman, A. I. Vainshtein and V. I. Zakharov, Nucl. Phys. B **166** (1980) 493

[12] M. Dine, W. Fischler and M. Srednicki, Phys. Lett. B **104** (1981) 199

[13] A. R. Zhitnitsky, Sov. J. Nucl. Phys. **31** (1980) 260

[14] M. Gorghetto, E. Hardy and G. Villadoro, SciPost Phys. **10** (2021) 050

[15] A. Ringwald and K. Saikawa, Phys. Rev. D **93** (2016) 085031

[16] K. A. Beyer and S. Sarkar, SciPost Phys. **15** (2023) 003

[17] M. Kamionkowski and J. March-Russell, Phys. Lett. B **282** (1992) 141

[18] R. Holman *et al.*, Phys. Lett. B **282** (1992) 136

[19] S. M. Barr and D. Seckel, Phys. Rev. D **46** (1992) 549

[20] Q. Lu, M. Reece and Z. Sun, JHEP **07** (2024) 227

[21] A. Caputo and G. Raffelt, PoS **COSMICWISPers** (2024) 041

[22] V. Anastassopoulos *et al.* [CAST], Nature Phys. **13** (2017) 590

[23] F. T. Avignone, III *et al.* [SOLAX], Phys. Rev. Lett. **81** (1998) 5071

[24] R. Bernabei *et al.*, Phys. Lett. B **515** (2001) 12

[25] A. Morales *et al.* [COSME], Astropart. Phys. **16** (2002) 332

[26] Z. Ahmed *et al.* [CDMS], Phys. Rev. Lett. **103** (2009) 141802

[27] P. Belli *et al.*, Phys. Lett. B **711** (2012) 45

[28] E. Armengaud *et al.*, JCAP **11** (2013) 067

[29] I. J. Arnquist *et al.* [Majorana], Phys. Rev. Lett. **129** (2022) 081803

[30] E. Aprile *et al.* [XENON], Phys. Rev. Lett. **129** (2022) 161805

[31] J. B. Dent, B. Dutta and A. Thompson, JHEP **02** (2024) 190

[32] J. Jaeckel, E. Masso, J. Redondo, A. Ringwald and F. Takahashi, Phys. Rev. D **75** (2007) 013004

[33] P. Carenza, M. Giannotti, J. Isern, A. Mirizzi and O. Straniero, Phys. Rept. **1117** (2025) 1

[34] K. Springmann, M. Stadlbauer, S. Stelzl and A. Weiler, arXiv:2410.19902 [hep-ph]

[35] P. Astier *et al.* [NOMAD], Phys. Lett. B **479** (2000) 371

[36] J. P. Lees *et al.* [BaBar], Phys. Rev. Lett. **119** (2017) 131804

[37] M. J. Dolan, T. Ferber, C. Hearty, F. Kahlhoefer and K. Schmidt-Hoberg, JHEP **12** (2017), 094 [erratum: JHEP **03** (2021) 190]

[38] D. Banerjee *et al.* [NA64], Phys. Rev. Lett. **125** (2020) 081801

[39] J. W. D. Halliday *et al.*, Phys. Rev. Lett. **134** (2025) 055001

[40] C. Robilliard *et al.*, Phys. Rev. Lett. **99** (2007) 190403

[41] K. Ehret *et al.*, Phys. Lett. B **689** (2010) 149

[42] R. Ballou *et al.* [OSQAR], Phys. Rev. D **92** (2015) 092002

[43] W. Liao, Phys. Lett. B **702** (2011) 55

[44] W. Buchmuller and F. Hoogeveen, Phys. Lett. B **237** (1990) 278

[45] T. Yamaji, T. Yamazaki, K. Tamasaku and T. Namba, Phys. Rev. D **96** (2017) 115001

[46] `https://x-server.gmca.aps.anl.gov/x0h.html`

[47] T. Yamaji, K. Tamasaku, T. Namba, T. Yamazaki and Y. Seino, Phys. Lett. B **782** (2018) 527

[48] F. Della Valle *et al.*, arXiv:1410.4081 [hep-ex]

[49] R. Battesti *et al.*, Phys. Rev. Lett. **105** (2010) 250405

[50] T. Inada *et al.*, Phys. Rev. Lett. **118** (2017) 071803